Adaptive Model-Predictive-Control-Based Real-Time Energy Management of Fuel Cell Hybrid Electric Vehicles

Chao Jia, *Member, IEEE*, Wei Qiao, *Fellow, IEEE*, Junwei Cui, *Member, IEEE*, and Liyan Qu, *Senior Member, IEEE*

***Abstract*—To compete with battery electric vehicles, fuel cell (FC) hybrid electric vehicles (FCHEVs) are required to offer better performance in fuel economy and FC durability. To this end, this article proposes a novel real-time adaptive model predictive control (AMPC)-based energy management strategy (EMS) for FCHEVs to improve their fuel efficiency and mitigate the degradation of their onboard FC hybrid systems. First, a linear parameter-varying (LPV) prediction model of the FC hybrid system that considers the system parameter variation is developed. The model offers sufficient accuracy while enabling the real-time implementation capability of the AMPC. Then, an AMPC strategy is proposed to optimally distribute the load current of the FCHEV between the FC and the battery in real time. In each control interval of the AMPC, the LPV prediction model is updated online to adapt to the variations of the battery state of charge. The constrained optimization problem of the AMPC is then formulated to achieve a desired tradeoff among four performance metrics and is further transformed into a quadratic programming problem, which can be solved in real time. Hardware-in-the-loop tests are performed on a downscaled FC hybrid system with the proposed AMPC-based EMS, a commonly used rule-based EMS, an equivalent consumption minimization strategy, and an improved MPC-based EMS, respectively. Results show that among the four real-time EMSs, the AMPC-based EMS achieves the best performance in reducing hydrogen consumption and FC current fluctuation and the smallest optimality gap with respect to an offline dynamic programming-based optimal EMS.**

***Index Terms*—Adaptive model predictive control (AMPC), battery, energy management strategy (EMS), fuel cell hybrid electric vehicle (FCHEV), real time.**

I. Introduction

THANKS to the merits of zero emission, short refueling time, and high energy conversion efficiency, fuel cell (FC) hybrid electric vehicles (FCHEVs) are widely regarded as one of the most promising solutions to the air pollution problem caused by the ever-increasing usage of fossil fuels in transportation [1], [2]. After extensive research and development efforts, various models of commercially available FCHEVs, such as Toyota Mirai, Hyundai Nexo, and Honda Clarity Fuel Cell, have been launched in recent years [3].

An FCHEV commonly employs a proton exchange membrane (PEM) FC (PEMFC) stack as the main power source and a battery pack or/and a supercapacitor (SC) as the secondary power source [4]. For the sake of conciseness, the onboard power system comprising an FC system (FCS) with a secondary power source is referred to as the FC hybrid system in this article. The second power source plays an important role in mitigating the issue of slow dynamic response of the FCS, capturing the regenerative braking energy, and providing electrical power for the balance of plant during the startup of the FCS.

The hybridization of two power sources requires a dedicated energy management strategy (EMS) for the supervisory control of the FC hybrid system [5]. The EMS is responsible for splitting the demand power or load current of the FCHEV between the power sources and controlling the power sources to respect their constraints. Since the power sources of the FC hybrid system have distinct properties in the power performance, efficiency, and degradation rate [4], the EMS should be properly designed to achieve the desired real-time performance of the FC hybrid system.

A variety of EMSs have been proposed for FCHEVs to 1) reduce the hydrogen consumption and improve the energy efficiency of the FC hybrid system, 2) mitigate the performance degradation of the FC stack, 3) reduce the degradation of the battery, and 4) enhance the reliability and cost effectiveness. These existing EMSs can be classified into two categories: rule-based and optimization-based strategies. The deterministic-rule-based EMSs typically employ the state-machine technique in which a set of rules are designed to control the FC hybrid system based on the states of the power sources and vehicle operation modes [6], [7]. Owing to the simplicity in the decision making for complex systems, fuzzy-logic-based EMSs were investigated in [8] and [9] for FCHEVs. Another important group of the rule-based EMSs are the frequency-decoupling strategies [10], [11]. The idea behind these strategies is to let the battery supply

Manuscript received 13 May 2022; revised 22 August 2022; accepted 8 October 2022. Date of publication 14 October 2022; date of current version 18 November 2022. This work was supported in part by the U.S. National Science Foundation under CAREER Award ECCS-1554497, and in part by the Nebraska Public Power District through the Nebraska Center for Energy Sciences Research. Recommended for publication by Associate Editor A. Barrado. *(Corresponding author: Wei Qiao.)*

The authors are with the Power and Energy Systems Laboratory, Department of Electrical and Computer Engineering, University of Nebraska-Lincoln, Lincoln, NE 68588-0511 USA (e-mail: cjia@huskers.unl.edu; wqiao3@unl.edu; Junwei.Cui@huskers.unl.edu; lqu2@unl.edu).

Color versions of one or more figures in this article are available at https://doi.org/10.1109/TPEL.2022.3214782.

Digital Object Identifier 10.1109/TPEL.2022.3214782

the high-frequency component of the load current and to allocate the low-frequency component of the load current to the FCS. These rule-based EMSs are capable of real-time implementation but have a disadvantage of being difficult to explicitly consider the performance metrics of the FC hybrid system [12]. As a result, the control performance of the rule-based EMSs is usually far away from the optimum in terms of the predefined control objectives of the FC hybrid system.

To overcome the nonoptimal performance of the rule-based EMSs, optimization-based EMSs have been studied for FC hybrid systems. The optimization-based EMSs were commonly developed by using the dynamic programming (DP) technique, which offers global optimal solution. For instance, DP was employed in [13] to minimize a complicated multiobjective cost function, which comprises the costs of the hydrogen consumption, electric energy consumption, frequent start–stop of the FCS, etc. However, DP is impeded by the requirement for the prior knowledge of the entire driving cycle and heavy computational burden [14]. For example, a well-known issue of DP is the "curse of dimensionality," which is caused by the exponential increase in the processing time and storage space required to compute the solution via DP as the dimension of the problem space (i.e., the number of state and control variables) increases. Thus, DP is not capable of real-time optimal energy management for the FC hybrid system. Hu et al. [15] proposed another global optimal EMS for FCHEVs using the convex optimization technique, which is much more computationally efficient than DP. However, since the convex optimization can only solve the problems with convex objective functions over convex sets, the model of the FCHEV must be simplified significantly to ensure the convexification. As the consequence, the optimality of the solution may degrade [16]. Furthermore, the EMS based on the convex optimization requires knowing the whole driving cycle in advance and, thus, cannot be used for real-time optimal energy management.

Model predictive control (MPC)-based strategies have been reported in the literature for real-time energy managements of FC hybrid systems [16], [17], [18], [19], [20], [21], [22]. The MPC makes explicit use of a prediction model to predict the future states and outputs of the controlled system to obtain the optimal control actions by minimizing a cost function, which is related with the future states and outputs of the system. The duration from the current time instant to the future time instant at which the prediction of the system behavior is made is referred to as the prediction horizon. One significant advantage of the MPC strategies is that they can inherently cope with the hard constraints on the state and input variables [23].

Greenwell et al. [17] presented an MPC approach to optimize the current allocation of an FC/SC hybrid system. The control objective was to meet the power demand while minimizing the FCS power deviations from the point with the maximum efficiency. However, since the FCS in an FCHEV should be controlled to offer a broad range of the output power to satisfy various driving conditions but the FCS in [17] can only be operated within a very narrow power range around the maximum efficiency point, the strategy cannot be successfully applied to FCHEVs. Pereira et al. [18] proposed a nonlinear MPC for the energy management of FCHEVs in which a recurrent neural network was employed as the prediction model of the FCS. A downscaled hardware-in-the-loop (HIL) test setup was built to verify the MPC. The setup only included an FCS but did not include the battery or the dc–dc converter. Chen et al. [19] presented an improved MPC (IMPC)-based optimal EMS for FCHEVs. To enhance the control performance of the traditional MPC, the IMPC-based EMS employed the partial least square technique to forecast the load current of the FCHEV. Real-time experiment results were provided, but the regenerative braking, which is a critical function for efficiency improvement of the FCHEVs, was not considered in the IMPC or evaluated in the experiment. He et al. [20] proposed another MPC-based EMS to minimize the hydrogen consumption with the constraints on the FC output power fluctuations, battery state of charge (SOC), and FC temperature. The real-time performance of the EMS was obtained using an HIL experiment that only included the hardware of the controller. Based on the MPC, Hu et al. [16] proposed a novel cost-optimal EMS using an FC/battery health-aware predictive control. Zhou et al. [21] presented a multimode predictive EMS for FCHEVs using a Markov driving pattern recognizer. Shen et al. [22] presented a robust fuzzy MPC scheme with the T-S fuzzy modeling method to optimize the power distribution of the FCHEVs. Extensive simulation studies and discussions were provided in [16], [21], and [22], but no real-time validation or experiment test was performed. Since the MPC usually requires high computational resources, the real-time implementation of the MPC-based EMSs for FC hybrid systems is still a challenging task and requires computational-efficient MPC strategies.

As the cornerstone of the MPC, the prediction model should not only offer accurate predictions for the states and outputs of the plant, but also be simple to alleviate the computational burden incurred by solving the optimization problem of the MPC. Previous articles [16], [18], [20], [21], [22] used nonlinear prediction models, which led to complicated nonlinear constrained optimization problems that were difficult to solve in real time. Although the successive linearization approach has been used to linearize the nonlinear prediction model at each sampling time of the controller, the linearization inevitably leads to extra prediction errors and more computational cost and, thus, impedes the real-time implementation of the MPC strategies that use nonlinear prediction models.

In contrast to the nonlinear prediction models and conventional MPC formulation used in the existing EMSs [16], [17], [18], [19], [20], [21], [22], this article proposes a new EMS based on an adaptive MPC (AMPC) for FCHEVs. The prediction model of the AMPC-based EMS is represented by a linear parameter-varying (LPV) system, which is linear in the state space but nonlinear in the parameter space [24]. The LPV prediction model provides the sufficient accuracy while enabling the real-time implementation capability of the AMPC. In each control cycle of the AMPC, the parameters of the prediction model are updated online to adapt to the variations of the battery SOC. The cost function of the AMPC-based EMS includes four performance metrics: the hydrogen consumption, FC current fluctuations, battery power losses, and battery charge-sustaining.

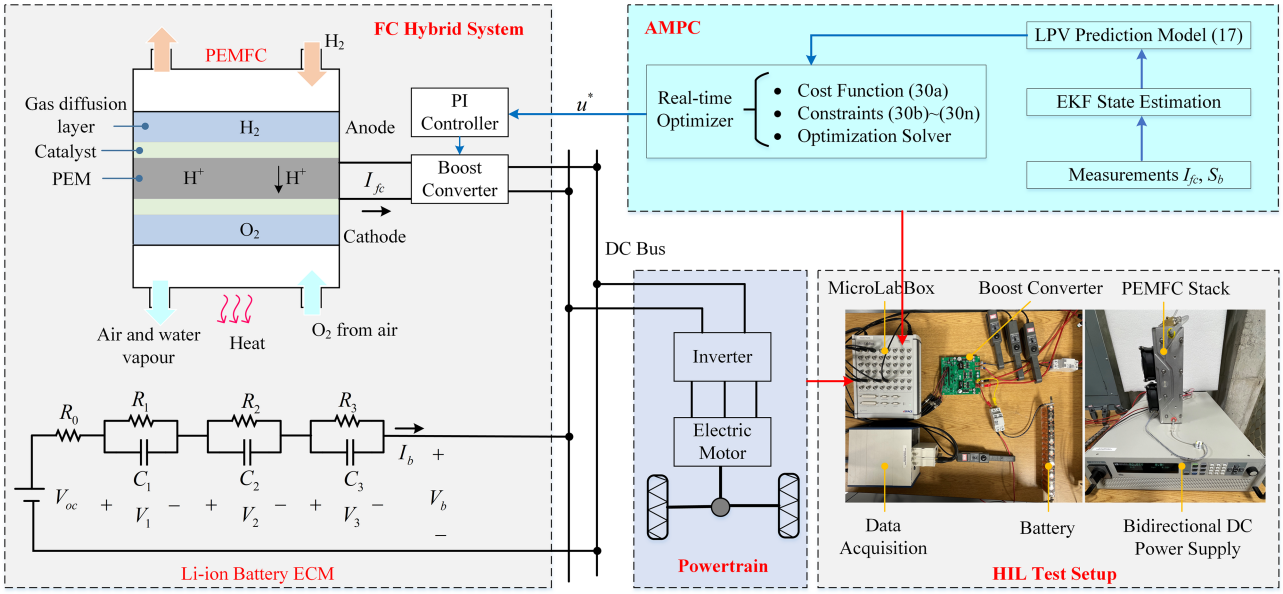

Fig. 1. Configuration of an FCHEV with the proposed AMPC-based EMS and HIL test setup.

The constrained optimization problem of the AMPC is formulated to achieve a tradeoff among these objectives and is further converted to a quadratic programming (QP) problem that can be solved online efficiently. By solving the QP problem online, the optimal current split between the two sources of the FC hybrid system is attained in real time. A comparative study is performed on a downscaled FC hybrid system via HIL tests to demonstrate that the AMPC-based EMS achieves better performance in reducing the energy consumption and FC current fluctuations than other three state-of-the-art real-time EMSs. Since the DP-based EMS cannot be implemented in real time, the simulation results of the offline DP-based optimal EMS are provided as a benchmark for the four real-time EMSs in the comparative study. The main contributions of this article are summarized as follows:

1) To the best of the authors' knowledge, this is the first EMS based on the MPC method that is capable of real-time energy management for FCHEVs while being adaptive to the nonlinearity of the system dynamics, which is achieved by using an LPV prediction model of the FC hybrid system in the proposed EMS. The experiment results demonstrate the superiority of the proposed EMS over other three real-time EMSs reported in recent literatures [19], [40].
2) Compared with the previous articles [16], [17], [18], [19], [20], [21], [22], this article developed a more complete HIL test setup for the FC hybrid system to experimentally validate the EMSs. An advantage of this setup over those in the previous articles is that it can test the optimal load current allocation when the energy of the FCHEV is being recovered by regenerative braking.
3) This article investigated the execution time of the proposed EMS with different prediction horizons using an embedded real-time simulator and determined the best prediction horizon based on the investigation. Such an investigation was not conducted in any of the previous articles [16], [17], [18], [19], [20], [21], [22].

The rest of the article is organized as follows. Section II introduces the plant model of the FC hybrid system. Section III presents the proposed AMPC-based EMS for FCHEVs. Parameter identification of the FC and battery models is presented in Section IV. Section V provides the real-time simulation evaluation of the proposed EMS. A comparative study of the proposed real-time EMS and three existing real-time EMSs using HIL testing and the offline DP-based optimal EMS as a benchmark is conducted in Section VI. Section VII draws conclusions for this article.

II. Plant Model of FC Hybrid System

The structure of the studied system is shown in Fig. 1. The lithium-ion battery is passively connected to the dc bus while the FC is connected to the dc bus by a boost converter. The proposed AMPC-based EMS is a supervisory controller that splits the load current of the FCHEV between the FC and the battery. The proposed AMPC consists of three parts: a prediction model, a real-time optimizer, and a state estimator. The real-time optimizer consists of a cost function and the constraints, which form a constrained optimization problem as well as an optimization solver. The output of the AMPC is the reference current for the FC. A proportional–integral controller is used to control the boost converter to draw current from the FC at the reference value.

This section presents a plant model of the FC hybrid system, which consists of a semi-empirical model for the FC and an equivalent circuit model (ECM) for the battery. The plant model will be employed to develop the prediction model of the FC hybrid system.

A. Semi-Empirical FC Model

Due to the merits of high efficiency, fast dynamic response, and low operation temperature, the PEMFC is the prime candidate for vehicle applications. As shown in Fig. 1, the PEMFC consists of a PEM sandwiched by an anode electrode and a cathode electrode, catalyst layers, and gas diffusion layers. Hydrogen and oxygen are separately fed to anode and cathode channels, diffuse through the gas diffusion layers, and reach the catalytic layers, respectively [25]. The hydrogen molecule is split into protons and electrons at the catalytic layer of the anode, while the electrons flow through an external circuit. At the cathode, oxygen combines with the protons and electrons to produce water.

For the energy management purpose, the following semi-empirical model of the PEMFC described as follows is most widely used due to the high precision [4], [26]:

$$V_{\text{fc}} = N_{\text{cell}} \left(E_{\text{Nernst}} - V_{\text{act}} - V_{\text{ohmic}} - V_{\text{con}} \right) \tag{1}$$

$$E_{\text{Nernst}} = 1.229 - 8.5 \times 10^{-4} \left(T_{\text{fc}} - 298.15 \right) + 4.3085 \times 10^{-5} T_{\text{fc}} \left(\ln \left(P_{\text{H2}} \right) + \ln \left(\sqrt{P_{\text{O2}}} \right) \right) \tag{2}$$

$$\begin{cases} V_{\text{act}} = -\left[\xi_1 + \xi_2 T_{\text{fc}} + \xi_3 T_{\text{fc}} \cdot \ln \left(C_{\text{O2}} \right) + \xi_4 T_{\text{fc}} \cdot \ln \left(I_{\text{fc}} \right) \right] \\ C_{\text{O2}} = \frac{P_{\text{O2}}}{5.08 \times 10^6 \exp(-498/T_{\text{fc}})} \end{cases} \tag{3}$$

$$V_{\text{ohmic}} = I_{\text{fc}} R_{\text{int}} \tag{4}$$

$$V_{\text{con}} = -b \cdot \ln \left(1 - \frac{J}{J_{\text{max}}} \right) \tag{5}$$

where V_{fc} is the stack output voltage in V; N_{cell} is the number of cells in the stack; E_{Nernst} is the thermodynamic potential of the cell in V; V_{act} is the activation voltage drop in V; V_{ohmic} is the ohmic voltage drop; V_{con} is the concentration voltage drop; T_{fc} is the stack temperature in K; P_{H2} is the hydrogen partial pressure in N/m^2 at the anode side; P_{O2} is the oxygen partial pressure in N/m^2 at the cathode side; $\xi_n (n = 1, \cdots, 4)$ are the semi-empirical coefficients based on the fluid mechanics, thermodynamics, and electrochemistry of the PEMFC [4]; C_{O2} is the oxygen concentration in mol/cm^3; I_{fc} is the FC current in A; R_{int} is the internal resistor in Ω; b is a coefficient in V; J is the actual current density of the cell in A/cm^2; and J_{max} is the maximum current density in A/cm^2.

The hydrogen consumption rate $\dot{m}_{\text{H}_2}$ in g/s is expressed as follows [7], [27]:

$$\dot{m}_{\text{H}_2} = \gamma I_{\text{fc}} \tag{6}$$

where

$$\gamma = \frac{\rho s N_{\text{fc}-p} N_{\text{fc}-s}}{2 \varphi F} \tag{7}$$

where ρ is the molar mass of hydrogen in g/mol; s is the hydrogen stoichiometry; φ is the active surface area of a cell in cm^2; F is the Faraday constant; $N_{\text{fc}-s}$ is the number of cells in series; and $N_{\text{fc}-p}$ is the number of branches in parallel.

B. Battery Model

As illustrated in Fig. 1, the ECM of the battery comprises an open circuit voltage V_{oc}, a series resistance R_o, and three pairs of the resistor–capacitor (RC) branches R_n and C_n, where $n = [1, 2, 3]$. The RC pairs reflect the transient characteristic of the battery. The values of the eight parameters are dependent on the battery SOC, S_b. Such dependence will be specified by experimental testing and saved in lookup tables for the real-time application. The battery ECM is described by [28]

$$\dot{V}_n = \frac{I_b}{C_n} - \frac{V_n}{R_n C_n} \tag{8}$$

$$U_b = V_{\text{OC}} - I_b R_0 - \sum_{n=1}^{3} V_n \tag{9}$$

$$\dot{S}_b = -I_b / Q_b \tag{10}$$

$$P_{b,\text{Loss}} = I_b^2 R_0 + \sum_{n=1}^{3} \frac{V_n^2}{R_n} \tag{11}$$

where U_b, I_b, Q_b, and $P_{b,\text{Loss}}$ are the terminal voltage, current, nominal capacity, and power loss of the battery, respectively; V_n is the voltage across the nth RC pair; and a positive/negative current I_b indicates that battery is in the discharge/charge mode of operation.

III. Proposed AMPC-Based EMS

This section first develops a new LPV prediction model of the FC hybrid system in a state–space representation based on the plant model in Section II. A cost function is then defined according to the control objectives for the energy management of the FC hybrid system. A constrained optimization problem is formulated to minimize the cost function of the AMPC, which is further transformed into a QP problem. In each sampling interval, the optimal current allocation between the FC and the battery within the FC hybrid system is obtained by solving the QP problem online using an optimization solver. In addition, the unmeasured states in the state–space representation are estimated by the classic extended Kalman filter (EKF).

A. Prediction Model of FC Hybrid System

To develop the LPV prediction model of the FC hybrid system for the proposed AMPC, (8) and (10) are first discretized as follows using the zero-order hold method:

$$V_n (k+1) = \left(1 - \frac{T}{R_n (k) C_n (k)} \right) V_n (k) + \frac{T}{C_n (k)} I_b (k) \tag{12}$$

$$S_b (k+1) = S_b (k) + \frac{-T}{Q_b} I_b (k) \tag{13}$$

where k is the time index and T is the sampling interval. Similar to [19], the FC current can be expressed as

$$I_{\text{fc}} (k+1) = I_{\text{fc}} (k) + T \Delta I_{\text{fc}} (k) \tag{14}$$

where ΔI_{fc} is the slew rate of the FC current. According to (12)–(14), the state–space representation of the FC hybrid system can be derived in the following compact form:

$$x(k+1) = A(k)\,x(k) + B(k)\,u(k) \tag{15}$$

$$y(k) = Cx(k) \tag{16}$$

where$x \in \mathbb{R}^{n_x}$ is the state vector; $u \in \mathbb{R}^{n_u}$ is the input vector; $y \in \mathbb{R}^{n_x}$ is the output vector; and $A \in \mathbb{R}^{n_x \times n_x}$, $B \in \mathbb{R}^{n_x \times n_u}$, and $C \in \mathbb{R}^{n_x \times n_x}$ are the matrices of the state–space representation. These vectors and matrices are given by

$$x(k) = [I_{\text{fc}}(k), V_1(k), V_2(k), V_3(k), S_b(k)]'$$

$$u(k) = [\Delta I_{\text{fc}}(k), I_b(k)]'$$

$$A(k) = \begin{bmatrix} 1 & 0 & 0 & 0 & 0 \\ 0 & 1-\frac{T}{R_1(k)C_1(k)} & 0 & 0 & 0 \\ 0 & 0 & 1-\frac{T}{R_2(k)C_2(k)} & 0 & 0 \\ 0 & 0 & 0 & 1-\frac{T}{R_3(k)C_3(k)} & 0 \\ 0 & 0 & 0 & 0 & 1 \end{bmatrix}$$

$$B(k) = \begin{bmatrix} T & 0 \\ 0 & T/C_1(k) \\ 0 & T/C_2(k) \\ 0 & T/C_3(k) \\ 0 & -T/Q_b \end{bmatrix}, C = \mathbf{I}_{n_x}, n_x = 5, n_u = 2$$

where $\mathbf{I}_{n_x}$ represents a $n_x \times n_x$ identity matrix. $A(k)$ and $B(k)$ are dependent on the exogenous parameters $R_n(k)$ and $C_n(k)$, which vary with the battery SOC. Such a system is referred as an LPV system, which is linear in the state space, but nonlinear in the parameter space [24].

Given a predicted input sequence, the corresponding sequence of the state predictions is obtained by simulating (15) forward over the prediction horizon N_p recursively. For notational convenience, the predicted sequences are stacked into vectors $\mathbf{u}$ and $\mathbf{x}$, given by

$$\mathbf{u}(k) = \begin{bmatrix} u(k|k) \\ u(k+1|k) \\ \vdots \\ u(k+N_p-1|k) \end{bmatrix}, \mathbf{x}(k) = \begin{bmatrix} x(k|k) \\ x(k+1|k) \\ \vdots \\ x(k+N_p|k) \end{bmatrix},$$

where $k+i|k$ denotes the value of a variable or parameter predicted at time $k+i$ based on the information derived at time k; and $x(k+i+1|k)$ is governed by the prediction model

$$\begin{aligned} x(k+i+1|k) = {} & A(k+i|k)x(k+i|k) \\ & + B(k+i|k)\,u(k+i|k) \\ i \in {} & \{0, \cdots, N_p-1\} \end{aligned} \tag{17}$$

where the initial condition (at the start of the prediction horizon) is defined by

$$x(k|k) = x(k).$$

The state vector $x(k)$ includes unmeasured states, such as $V_1(k)$, $V_2(k)$, and $V_3(k)$, which are estimated online by using an EKF. The EKF is a popular state estimation method in battery applications. The implementation procedure of the EKF algorithm can be found in [29] and [30].

B. Control Objectives and Cost Function

The goal of the proposed AMPC-based EMS is to optimally allocate the load current between the FC and the battery to reach a desired tradeoff among four competing performance metrics: the hydrogen consumption $\ell_{m_{\text{H2}}}$, the FC current variation $\ell_{\Delta I_{\text{fc}}}$, the battery power loss $\ell_{P_{b,\text{Loss}}}$, and the battery SOC deviation from the reference value ℓ_{S_b}. These performance metrics are defined in a quadratic form as follows. The first performance metric $\ell_{m_{\text{H2}}}$ is defined to consider the hydrogen utilization efficiency

$$\ell_{m_{\text{H2}}}(k) = \Delta m_{\text{H2}}^2(k) \tag{18}$$

where $\Delta m_{\text{H2}}(k)$ is the consumed hydrogen mass at time k.

Due to slow response dynamics, the PEMFC is not capable of tracking rapid load variations. This is because fast varying load demand profiles may cause fuel starvation, membrane drying, flooding, and pressure imbalance across the FC membrane [31]. To avoid these issues, the change rate of the FC current is penalized according to the second performance metric $\ell_{\Delta I_{\text{fc}}}$ defined as follows [19].:

$$\ell_{\Delta I_{\text{fc}}}(k) = \Delta I_{\text{fc}}^2(k). \tag{19}$$

According to (11), the third performance metric $\ell_{P_{b,\text{Loss}}}$ is defined as

$$\ell_{P_{b,\text{Loss}}}(k) = I_b^2(k)\,R_0 + \sum_{n=1}^{3} \frac{V_n^2(k)}{R_n}. \tag{20}$$

Current commercially available FCHEVs, such as Toyota Mirai, Hyundai Nexo, and Honda Clarity, typically use a small-size battery pack for their onboard energy systems. Since the battery cannot be charged from the electric grid, the EMS is desired to control the onboard energy system to ensure the battery's charge sustaining [16], [32]. To this end, the last performance metric considers the deviation of the battery SOC from the reference value S_{ref} , given by

$$\ell_{S_b}(k) = (S_b(k) - S_{\text{ref}})^2. \tag{21}$$

The running cost function is defined as the weighted sum of the four performance metrics to achieve a desired tradeoff among them

$$\begin{aligned} L(x,u,k) = {} & \lambda_1 \ell_{m_{\text{H2}}}(k) + \lambda_2 \ell_{\Delta I_{\text{fc}}}(k) \\ & + \lambda_3 \ell_{P_{b,\text{Loss}}}(k) + \lambda_4 \ell_{S_b}(k) \end{aligned} \tag{22}$$

where λ_1, λ_2, λ_3, and λ_4 are weighting factors that can be adjusted to prioritize one objective over the others.

In addition to the performance metrics, some important constraints should be respected to operate the onboard energy system safely. To avoid the fuel starvation issue and protect the health of the FCS, the FC current and its variation rate are limited as follows [33]:

$$0 \le I_{\text{fc}}(k) \le I_{\text{fc,max}} \tag{23}$$

$$\Delta I_{\text{fc,min}} \le \Delta I_{\text{fc}}(k) \le \Delta I_{\text{fc,max}}. \tag{24}$$

The battery SOC is constrained by (25) to prevent the battery from both overcharge and overdischarge

$$S_{b,\min} \le S_b(k) \le S_{b,\max} \tag{25}$$

and the battery current is bounded by

$$I_{b,\min} \le I_b(k) \le I_{b,\max} \tag{26}$$

where (23)–(26) are hard constraints on state and input variables, which should be respected by the AMPC-based EMS.

C. Online Optimization Problem

In each sampling interval of the EMS, the AMPC solves a constrained optimization problem online to obtain the optimal sequence of the control variables ΔI_{fc} and I_b. The objective function of the optimization problem is the sum of the predicted running cost over the prediction horizon N_p, expressed as

$$\begin{aligned} J = \sum_{l=1}^{N_p} \Bigg(& \lambda_1 \ell_{m_{\text{H2}}}(k+l|k) + \lambda_3 \sum_{n=1}^{3} \frac{V_n^2(k+l|k)}{R_n(k+l|k)} \\ & + \lambda_4 \ell_{S_b}(k+l|k)) \\ & + \sum_{v=0}^{N_u-1} \left(\lambda_2 \ell_{\Delta I_{\text{fc}}}(k+v|k) + \lambda_3 I_b^2(k+v|k) R_0 \right) \end{aligned} \tag{27}$$

where N_u is the control horizon. Substituting (18)–(26) into (27), (27) can be rewritten as

$$\begin{aligned} J = & \sum_{l=1}^{N_p} \| Q(k+l|k) (x(k+l|k) - r) \|_2^2 \\ & + \sum_{v=0}^{N_u-1} \| R(k+v|k) \cdot u(k+v|k) \|_2^2 \end{aligned} \tag{28}$$

where $\| \cdot \|_2^2$ is the square of the Euclidean norm [18]; and Q and R are the weight matrices on the tracking errors and control efforts, respectively, given by

$$\begin{aligned} Q(k+l|k) = & \operatorname{diag}\Big(\gamma\sqrt{\lambda_1}, \sqrt{\lambda_3 / R_1(k+l|k)}, \\ & \sqrt{\lambda_3 / R_2(k+l|k)}, \sqrt{\lambda_3 / R_3(k+l|k)}, \sqrt{\lambda_4} \Big) \in \mathbb{R}^{n_x \times n_x}, \end{aligned}$$

and $R(k+v|k) = \operatorname{diag}(\sqrt{\lambda_2}, \sqrt{\lambda_3 R_0(k+v|k)}) \in \mathbb{R}^{n_u \times n_u}$; and $r = [0,0,0,0,S_{\text{ref}}]' \in \mathbb{R}^{n_x}$.

The optimization problem is then formulated as (29) to minimize (28) subject to linear constraints

$$\begin{aligned} \min_{\mathbf{u}(k)} & \sum_{l=1}^{N_p} \| Q(k+l|k) \cdot (x(k+l|k) - r) \|_2^2 \\ & + \sum_{v=0}^{N_u-1} \| R(k+v|k) \cdot u(k+v|k) \|_2^2 \end{aligned} \tag{29a}$$

subject to

$$\begin{aligned} x(k+i+1|k) = & A(k+i|k) x(k+i|k) \\ & + B(k+i|k) u(k+i|k) \end{aligned} \tag{29b}$$

$$\begin{aligned} & V_b(k+i|k) I_b(k+i|k) + \eta V_{\text{fc}}(k+i|k) I_{\text{fc}}(k+i|k) \\ & = V_b(k+i|k) I_l(k+i|k) \end{aligned} \tag{29c}$$

$$x(k|k) = x(k) \tag{29d}$$

$$x_{\min} \le x(k+i+1|k) \le x_{\max} \tag{29e}$$

$$u_{\min} \le u(k+i|k) \le u_{\max} \tag{29f}$$

$$i \in \{0, \cdots, N_p - 1\} \tag{29g}$$

where $\mathbf{u}(k) \in \mathbb{R}^{N_u n_u}$ is the vector of decision variables defined before (17); η is the efficiency of the boost converter; I_l is the load current of the FC hybrid system, which is typically considered as a measured disturbance in the energy management of FCHEVs [21]; $x_{\min}$ and $x_{\max}$ are the lower and upper bounds on the state variables, respectively; and $u_{\min}$ and $u_{\max}$ are the lower and upper bounds on the control variables, respectively. Considering the requirement of fulfilling the power demand of the FCHEV, the power balance on the dc bus, described by (29c), imposes equality constraints in the optimization problem. Since the battery needs to provide electrical power for the balance of plant during the startup of the FCS, the proposed EMS should prevent the battery from charge depletion. Thus, sustaining the battery SOC is considered in the objective function (29a) by minimizing its deviation from the reference SOC and in Constraint (29e), which limits the battery SOC variation range.

Over the prediction horizon, the variation of the battery SOC is very small, so do the parameter variations of the battery. Therefore, the varying parameters can be treated as fixed values over the prediction horizon in the AMPC formulation (29) namely, $A(k+i|k) = A(k|k) = A(k)$ and $B(k+i|k) = B(k|k) = B(k)$, for $1 \le i \le N_p$. As discussed in [24] and [34], such an approach makes the MPC much simpler to implement and run in real time. Then, (29) can be expressed as the following QP problem, which includes a quadratic cost function and linear constraints:

$$\min_{\mathbf{u}(k)} \frac{1}{2} \mathbf{u}'(k) H(k) \mathbf{u}(k) + h'(k) \mathbf{u}(k) \tag{30a}$$

subject to

$$G(k) \mathbf{u}(k) \le w(k) \tag{30b}$$

$$E(k) \mathbf{u}(k) = e(k) \tag{30c}$$

$$\begin{aligned} H(k) = & \phi'(k) \bar{Q}'(k) \bar{Q}(k) \phi(k) + \bar{R}'(k) \bar{R}(k), \\ & H(k) \in \mathbb{R}^{(N_u n_u) \times (N_u n_u)} \end{aligned} \tag{30d}$$

$$\begin{aligned} \bar{Q}(k) = & \operatorname{diag}(Q(k+1|k), \cdots, Q(k+N_p|k)), \\ & \bar{Q}(k) \in \mathbb{R}^{(N_p n_x) \times (N_p n_x)} \end{aligned} \tag{30e}$$

$$\begin{aligned} \bar{R}(k) = & \operatorname{diag}(R(k|k), \cdots, R(k+N_u-1|k)), \\ & \bar{R}(k) \in \mathbb{R}^{(N_u n_u) \times (N_u n_u)} \end{aligned} \tag{30f}$$

$$\phi(k) =$$

$$\begin{bmatrix} B(k) & 0 & 0 & 0 \\ A(k)B(k) & B & 0 & 0 \\ \vdots & \vdots & \ddots & 0 \\ A^{N_p-1}(k)B(k) & A^{N_p-2}(k)B(k) & \cdots & A^{N_p-N_u}(k)B(k) \end{bmatrix} \in \mathbb{R}^{(N_p n_x)\times(N_u n_u)} \tag{30g}$$

$$h(k) = \phi'(k)\bar{Q}(k)F(k)x(k) \in \mathbb{R}^{N_u n_u} \tag{30h}$$

$$F(k) = \begin{bmatrix} A(k) \\ A^2(k) \\ \vdots \\ A^3(k) \end{bmatrix} \in \mathbb{R}^{(N_p n_x)\times n_x} \tag{30i}$$

$$G(k) = \begin{bmatrix} -\psi \\ \psi \\ -\phi(k) \\ \phi(k) \end{bmatrix} \in \mathbb{R}^{2(N_u n_u + N_p n_x)\times N_u n_u} \tag{30j}$$

$$w(k) = \begin{bmatrix} -U_{\min} \\ U_{\max} \\ -X_{\min} \\ X_{\max} \end{bmatrix} \in \mathbb{R}^{2(N_u n_u + N_p n_x)} \tag{30k}$$

$$U_{\min} = \begin{bmatrix} u_{\min} \\ u_{\min} \\ \vdots \\ u_{\min} \end{bmatrix} \in \mathbb{R}^{N_u n_u}, \quad U_{\max} = \begin{bmatrix} u_{\max} \\ u_{\max} \\ \vdots \\ u_{\max} \end{bmatrix} \in \mathbb{R}^{N_u n_u} \tag{30l}$$

$$X_{\min} = \begin{bmatrix} x_{\min} \\ x_{\min} \\ \vdots \\ x_{\min} \end{bmatrix} \in \mathbb{R}^{N_p n_x}, \quad X_{max} = \begin{bmatrix} x_{\max} \\ x_{\max} \\ \vdots \\ x_{\max} \end{bmatrix} \in \mathbb{R}^{N_p n_x} \tag{30m}$$

$$\psi = \mathbf{I}_{(N_u n_u)} \in \mathbb{R}^{N_u n_u} \tag{30n}$$

where (30c) is a compact expression of equality constraints (29c).

When new states and measurements become available in a new sampling interval, the parameters of the prediction model (17) will be updated, leading to a parameter-varying prediction model. Consequently, the QP problem (30) of the AMPC will be adapted to the updated parameters in each sampling interval. Open-source or commercial solvers can be employed to solve (30) efficiently, which ensures the real-time implementation of the proposed AMPC-based EMS.

IV. Plant Model Parameter Identification

The coefficients of the FC semi-empirical model and the parameters of the battery ECM presented in Section II are determined by using experimental tests. Due to high price of the full-size FCSs using in FCHEVs, the previous articles [4], [18], [19] commonly employed downscaled experimental setups for the FC hybrid system, so did this article. The FC stack used in this article is from Horizon Fuel Cell Technologies, which has been used for studying FCHEVs in numerous literatures, such as [4], [26], and [35]. The major specifications of the FC stack are listed in Table I. The parameter identification of the FC model has been done in the authors' previous article [37]. Fig. 2 shows the voltage curves of the FC stack obtained from the experiment and the simulation using the FC model under the same dynamic load current condition. The output voltage obtained from the FC model agrees well with the experiment results, and the mean absolute percentage error is only 0.93% with respect to the experiment results.

TABLE I
Specifications of the FC Hybrid System

Specifications of the FC stack	
FC type	PEMFC
Number of cells	$N_{\text{cell}} = 24$
Rated power	500 W
Reactants	Hydrogen and air
Hydrogen pressure	0.45~0.55 bar
Hydrogen purity	≥ 99.995%
Cooling	Air (integrated cooling fan)
Humidification	Self-humidified
Cell active area	$\varphi = 77$ cm
Membrane thickness	38 μm
Specifications of the battery cell	
Battery type	$LiFePO_4$
Nominal voltage	3.3 V
Nominal capacity	1.1 Ah
Nominal energy	3.63 Wh

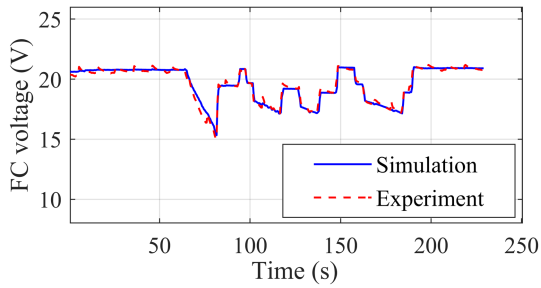

Fig. 2. Voltage curves of the FC stack obtained from the experiment and the simulation model.

In this article, the common pulse-rest test is carried out on a battery cell APR18650M1-B that is used in the battery pack of the FC hybrid system. The major specifications of the battery cell are provided in Table I. The cell is tested by using a Cadex C8000 Battery Tester. Based on the measurements of the cell voltage and current, the parameters of the battery ECM are extracted by the curve-fitting technique. Fig. 3 compares the voltage curves of the battery cell obtained from the pulse-rest test and the simulation using the ECM with identified parameters. The zoomed-in plots show two pulses of the voltage curves. The simulated battery voltage agrees perfectly with the experimental result. The mean absolute error between the model and the experimental result is only 2.1 mV, which is less than 0.1% of the measured voltage.

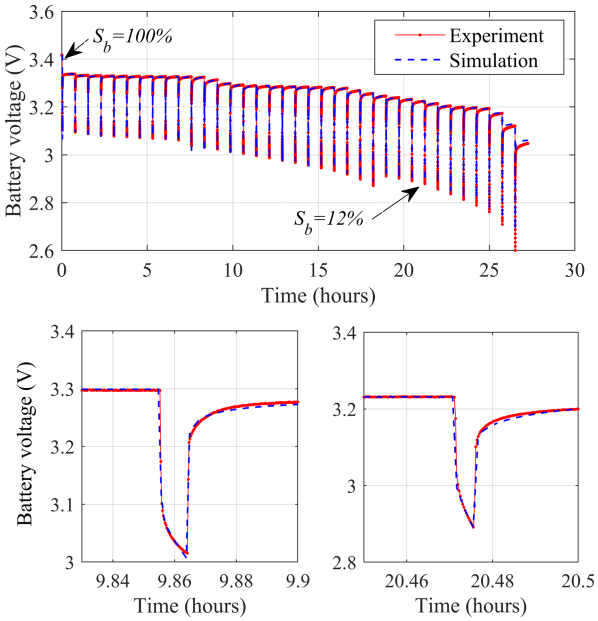

Fig. 3. Voltage curves of the battery cell obtained from the pulse-rest test and the ECM with identified parameters.

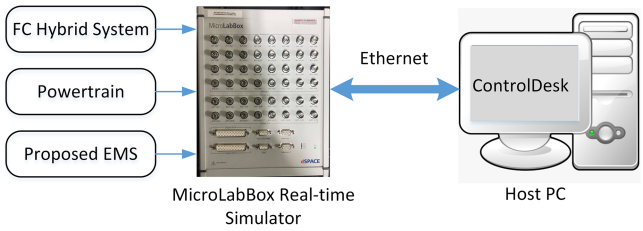

Fig. 4. Real-time simulation setup for the FCHEV.

V. Real-Time Simulation Evaluation

Real-time simulation provides flexible and fast meanings to evaluate, debug, and tune an EMS for an FCHEV. In this section, the real-time simulation setup of the studied FCHEV is introduced. Then, the execution time and control performance of the proposed AMPC-based EMS using different prediction horizons is evaluated using real-time simulation before it is applied to a physical plant. The length of the prediction horizon is then determined as a tradeoff of the execution time and control performance. Finally, this section presents how to determine the weighting factors of the cost function (27).

A. Real-Time Simulation Setup

The real-time simulation setup is shown in Fig. 4, where a dSPACE MicroLabBox is used as a real-time digital simulator to verify the real-time execution capability of the proposed EMS for an FCHEV. The MicroLabBox uses a 2 GHz, dual-core processor NXP QorIQ P5020 and communicates with a host personal computer (PC) via Gigabit Ethernet. Control Desk, the experiment and visualization software for the dSPACE real-time hardware platform, is executed on the host PC to monitor and control the simulation process.

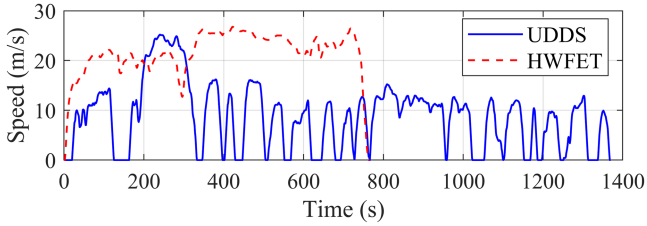

Fig. 5. Speed profiles of the UDDS and HWFET.

A simulation model of the FCHEV, which consists of an FC hybrid system model, a powertrain model, and the AMPC-based EMS, as shown in Fig. 1, is developed in MATLAB/Simulink and then implemented in the dSPACE MicroLabBox for the real-time simulation evaluation of the proposed EMS. The model of the FC hybrid system was described in Section II and their parameters were extracted in Section IV. The powertrain model was introduced in the authors' previous article [37]. The sampling intervals of the EMSs of hybrid vehicles are commonly set as 1 s [16], [31], which is adopted in this article. Two standard driving cycles, the Urban Dynamometer Driving Schedule (UDDS) and the Highway Fuel Economy Test (HWFET) cycle, whose speed profiles are illustrated in Fig. 5, are used for the FCHEV to evaluate the control performance of the proposed EMS. These two driving cycles are recommended by the U.S. Environmental Protection Agency for the fuel economy testing of light-duty vehicles.

B. Prediction Horizon Selection for the Proposed EMS

It is well known that MPC suffers from heavy computational burden. To ensure real-time implementation of an MPC algorithm in an embedded vehicle controller, it is necessary to know its execution time. In this article, the execution time of the MPC is the elapsed time from receiving new measurements to obtaining the optimal control action between two successive sampling instants of the EMS implemented in the embedded controller. The execution time is mainly determined by solving the online optimization problem, which depends on the complexity of the prediction model, the optimization solver, and the length of the prediction horizon. A longer prediction horizon usually leads to better control performance but higher computational burden due to the need for handling more decision variables in the optimization problem. This article determines the prediction horizon of the proposed AMPC-based EMS as a tradeoff between its execution time and control performance.

Previous articles on the MPC-based EMSs [15], [16], [17], [18], [19], [20] did not investigate the relationship between the execution time and the prediction horizon of the MPC. This article bridges this gap by evaluating the execution time of the AMPC implemented in the MicroLabBox using different prediction horizons. The execution time in MicroLabBox is also called the turnaround time and can be measured directly. The proposed AMPC-based EMS is evaluated over the UDDS

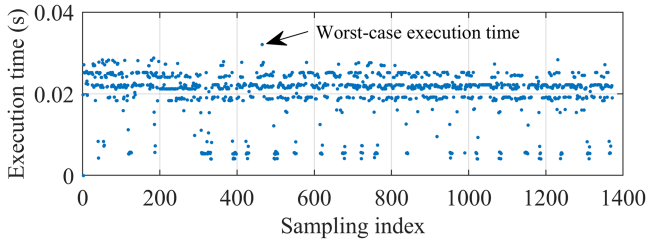

Fig. 6. Execution time of the AMPC-based EMS under the UDDS cycle when the prediction horizon is 3.

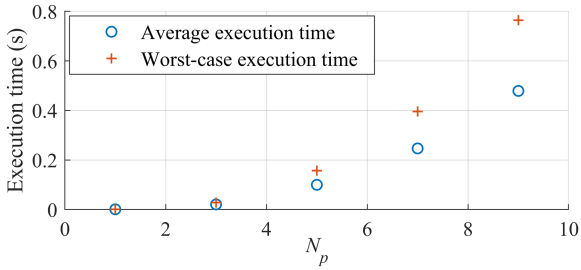

Fig. 7. Execution time of the AMPC-based EMS using different prediction horizons.

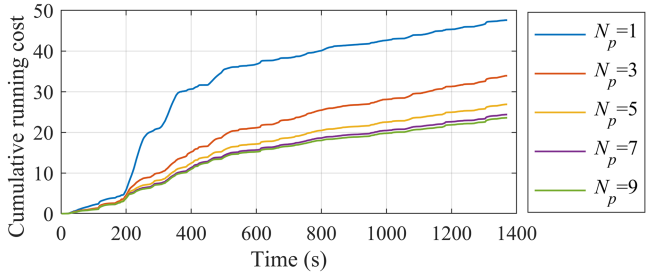

Fig. 8. Comparison of the cumulative running cost of the FCHEV over the UDDS cycle using the proposed EMS with different prediction horizons.

cycle. Fig. 6 shows the execution time of the EMS when the prediction horizon is 3 (i.e., 3 s). The measured turnaround time of the AMPC-based EMS varies from one sampling period to another. Among the measurements, the longest one is referred to as the worst-case execution time. Fig. 7 shows that both the average execution time and the worst-case execution time of the AMPC-based EMS grow almost quadratically with the increase of the prediction horizon N_p. When N_p is 10, the worst-case execution time is larger than the sampling interval of 1 s, indicating that the task of the AMPC-based EMS cannot complete in real time in the MicroLabBox. Thus, the prediction horizon should be smaller than 10 for the proposed AMPC-based EMS to be implemented in the MicroLabBox.

Fig. 8 shows that as the length of the prediction horizon N_p increases from 1 to 5, the cumulative running cost of the FCHEV defined by (22) over the UDDS cycle using the proposed EMS reduces significantly. However, when $N_p \geq 5$, the cumulative running cost only decreases slightly as N_p increases. On the other hand, the computational time grows significantly with the increase of N_p , as shown in Fig. 7. Thus, the prediction horizon is chosen to be 5 in this article.

C. Weighting Factor Selection for the Proposed EMS

The previous articles on the MPC-based EMSs for FCHEVs [16], [17], [21] either did not explain how to select the weighting factors or simply determine the weighting factors based on the authors' experience [19]. In contrast to these articles, this article selects the weight factors of the cost function (27) using the entropy weight method (EWM), which is widely used in multiobjective optimization problems [32], [41]. Since the four performance metrics considered in (27) have different orders of magnitude in value, they are first normalized with respect to the square of their nominal values [36], respectively. Then, based on the procedure in [36], λ_j is selected from a candidate set $\{0.1,\ 0.25,\ 0.5\}$, where $j = \{1,\ 2,\ 3,\ 4\}$, so there are 81combinations of the weighting factors. Since the two cases with $\lambda_1 = \lambda_2 = \lambda_3 = \lambda_4 = 0.1$ and $\lambda_1 = \lambda_2 = \lambda_3 = \lambda_4 = 0.5$, respectively, are the same as the case with $\lambda_1 = \lambda_2 = \lambda_3 = \lambda_4 = 0.25$, a total of 79 combinations of the weighting factors are tested using real-time simulation for the AMPC-based EMS. According to the value of each performance metric calculated directly by using (18)–(21), an evaluation matrix D is formed as follows:

$$D = \begin{bmatrix} d_{11} & \cdots & d_{1j} \\ \vdots & \ddots & \vdots \\ d_{i1} & \cdots & d_{ij} \end{bmatrix}$$

where d_{ij} is the value of the jth performance metric using the ith combination of the weighting factors.

Then, the weighting factors can be determined as follows of the EWM:

$$r_{ij} = \frac{d_j}{d_{ij}} \tag{31}$$

where d_j is the minimum value of the jth column of D.

Then, the entropy of the jth performance metric is given by

$$E_j = -\frac{1}{\ln(N)} \sum_{i=1}^{N} \mathrm{Pr}_{ij} \ln(\mathrm{Pr}_{ij}) \tag{32}$$

where $\mathrm{Pr}_{ij} = r_{ij} / \sum_{i=1}^{N} r_{ij}$ and $N = 79$ is the number of total combinations of weighting factors.

At last, λ_j is calculated by

$$\lambda_j = |1 - E_j| \Big/ \sum_{j=1}^{4} |1 - E_j| . \tag{33}$$

According to (33), the weighting factors are computed as $\lambda_1 = 0.1044$, $\lambda_2 = 0.6467$, $\lambda_3 = 0.0932$, and $\lambda_4 = 0.1557$. More detailed description and application examples of the EWM can be found in [41].

VI. Comparative Study via HIL Testing

This section first describes the downscaled HIL experiment setup for the FC hybrid system. A comparative study is then

carried out to validate the proposed EMS in comparison with three existing real-time EMSs based on the HIL experimental testing. In addition, the four real-time EMSs are compared with an offline DP-based optimal EMS, which was commonly used as the benchmark to evaluate the optimality of other EMSs for FCHEVs [20].

A. HIL Test Setup of the FC Hybrid System

As discussed in Section I, real-time simulation validation or HIL test was not performed in [16], [21], and [22]. The HIL setup in [18] did not include the battery or booster converter. The HIL setup in [19] cannot test the performance under the regenerative braking mode, and the HIL setup in [20] only employed the controller hardware. In comparison with these prior articles on MPC-based EMSs, the HIL setup for the FCHEV developed in this article is more complete for the FC hybrid system.

As shown in Fig. 1, the EMS and the powertrain simulation model of the FCHEV are implemented in the MicroLabBox, while the hardware is a downscaled FC hybrid system. The battery of the hybrid FCS consists of 16 APR18650M1-B cells tested in Section IV, which are connected in series. The FCS is a 500 W PEMFC stack, which is tied to the dc bus with a boost converter. A data acquisition system (NI SCXI-1305) stores the measurements of the FC current, the battery current, and the load current on the dc bus. A bidirectional dc power supply is controlled to mimic the electrical load on the dc bus for the traction and regenerative braking modes of the FCHEV.

B. Comparative Study and Discussions

The proposed EMS is compared with three existing real-time EMSs, including an IMPC-based EMS [19], a bounded load following strategy (BLFS) [40], and the equivalent consumption minimization strategy (ECMS) [40], by using the HIL-based experimental testing. As mentioned in Section I, the IMPC-based EMS does not take the parameter variation of the prediction model into consideration, so its prediction model is time-invariant. The BLFS is a rule-based EMS commonly used as the benchmark in the literature [4].The BLFS was designed to operate the FCS within multiple modes based on the battery SOC value and demand power, which enables the FCS to work in the high-efficiency region while alleviating the battery current. To operate the FCS to achieve a high efficiency, the FCS output power is bounded by two limits that can be adjusted according to the efficiency curve of the FCS. To alleviate the battery current, the FCS is operated in the power tracking mode [40]. In the ECMS, the power distribution is achieved by minimizing an instantaneous cost function that consists of the fuel consumption of the FCS and the equivalent fuel consumption of the battery. This article employs the ECMS used in [40] in which a weighting factor is introduced to adjust the control performance from the maximum fuel economy to the maximum care of the battery.

Since the DP method can offer an offline global optimal solution to the energy management problem of the FCHEV if assuming that the exact information of the driving cycle (e.g., speed, road slope, etc.) is known *a priori*, this article also provides the simulation results of the offline DP-based EMS as the benchmark in the comparative study. However, it should be pointed out that if the real-world driving cycle is slightly different from the prior knowledge of the driving cycle used for designing the DP-based EMS, its control performance will be nonoptimal. Furthermore, the DP-based EMS cannot be implemented in real time due to the heavy computational cost. Although these two shortcomings impeded the application of the DP-based EMS, it is commonly used as a benchmark to evaluate the control performance of other EMSs [20], [42].

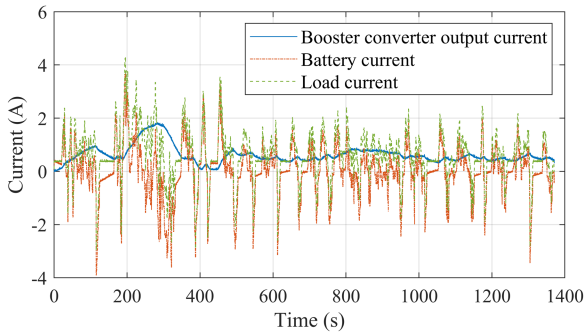

Fig. 9. Current allocation results of the FCHEV using the proposed AMPC-based EMS under the UDDS cycle.

According to Bellman's Principle of Optimality, the DP-based EMS minimizes a cost-to-go function $J_{N-k,\,N}$ from the current time step $N-k$ to the last time step N of a driving cycle to obtain the optimal control action at each discrete state of the FC hybrid systemby proceeding (34) backward in time recursively from the terminal cost $J^*_{N,N}$ defined by (35) [38]

$$\begin{aligned} &J^*_{N-k,\,N}\left(x\left(N-k\right)\right) \\ &\quad = \min_{u(N-k)} \left\{L\left(x\left(N-k\right), u\left(N-k\right), N-k\right)\right. \\ &\qquad \left. + J^*_{N-(k-1),N}\left(x\left(N-k+1\right)\right)\right\} \end{aligned} \tag{34}$$

$$J^*_{N,N}\left(x\left(N\right)\right) = L\left(x\left(N\right), u\left(N\right), N\right) \tag{35}$$

where $J^*_{N-k,\,N}$ is the minimum cost-to-go from the time step $N-k$ to N; L is the running cost function (22); and x and u are the state vector and input vector of the FC hybrid system, respectively, which were defined in Section II-A. A widely used DP toolbox [39] is employed to solve the optimization problem (34). This article uses the offline simulation results of the DP-based optimal EMS as the benchmark to evaluate the optimality of the four real-time EMSs implemented on the HIL test setup.

For the proposed EMS, the battery SOC reference S_{ref} is 0.7 [21]. Besides, the proposed EMS is required to satisfy the constraints (23)–(26) with the following limits for the FC hybrid system: $I_{\text{fc,max}} = 38$ A, $\Delta I_{\text{fc,min}} = -5$ A/s, $\Delta I_{\text{fc,max}} = 5$ A/s, $S_{b,\text{min}} = 0.5$, $S_{b,\text{max}} = 0.9$, $I_{b,\text{min}} = -25$ A, and $I_{b,\text{max}} = 25$ A.

Figs. 9 and 10 show the current allocation results of the FCHEV using the proposed AMPC-based EMS under the UDDS cycle and the HWFET cycle, respectively. Although the load current of the FCHEV varies significantly due to the repetitive acceleration and braking, the output current of the FC boost converter changes quite slowly. The battery assists the FC in

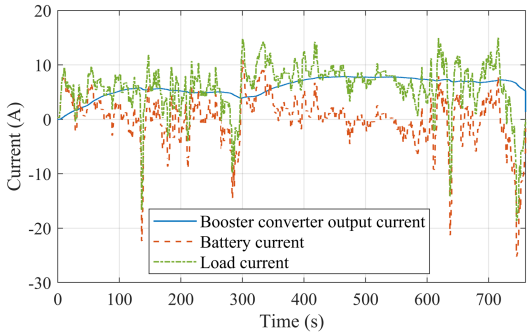

Fig. 10. Current allocation results of the FCHEV using the proposed AMPC-based EMS under the HWFET cycle.

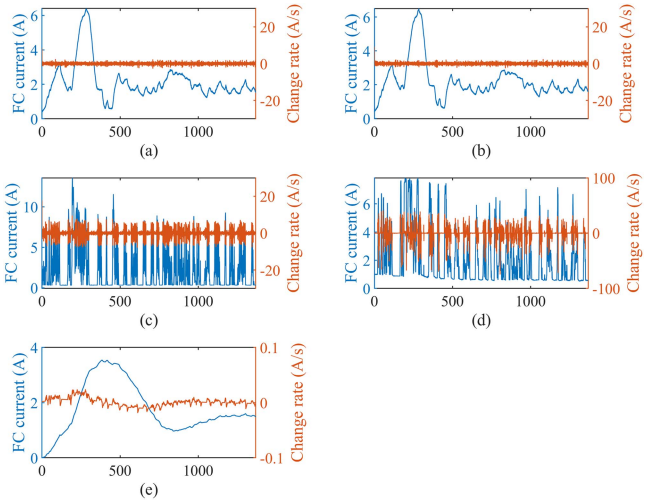

Fig. 11. FC current and its rate of change of the FCHEV using (a) proposed AMPC-based EMS, (b) IMPC-based EMS, (c) ECMS, (d) BLFS, and (e) DP-based EMS under the UDDS cycle.

shaving its peak current during the aggressive acceleration and, thus, mitigates the degradation of the FC. During the aggressive braking, the load current on the dc bus is negative; the battery absorbs the regenerative power of the FCHEV, which can reduce the energy consumption of the FCHEV. According to the load power of the UDDS cycle and HWFET cycle, the regenerative braking can reduce the total load power of the FCHEV by 18.98% and 6.84%, respectively. Since the UDDS is an urban driving cycle with more frequent acceleration and deceleration, the regenerative braking plays a more impressive role in the UDDS.

Figs. 11 and 12 compare the FC current of the FCHEV and its rate of change using the five EMSs under the UDDS and HWFET cycles, respectively. Compared with the BLFS and ECMS, the AMPC- and IMPC-based EMSs can make the output current of the FC much smoother by minimizing the objective function (22) over the prediction horizon and, therefore, significantly reduced the rate of the change of the FC current. The instantaneous cost function of the ECMS proposed in [40] only considers the fuel economy and battery current variation rather than the FC current variation. Thus, the change rate of the FC current using the

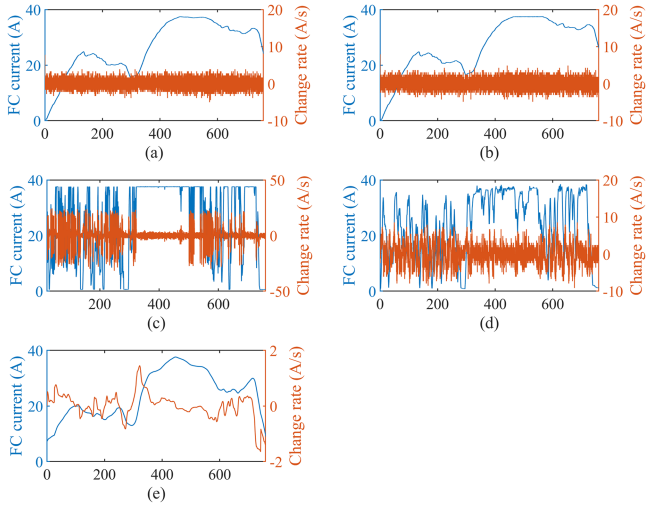

Fig. 12. FC current and its rate of change of the FCHEV using (a) proposed AMPC-based EMS, (b) IMPC-based EMS, (c) ECMS, (d) BLFS, and (e) DP-based EMS under the HWFET cycle.

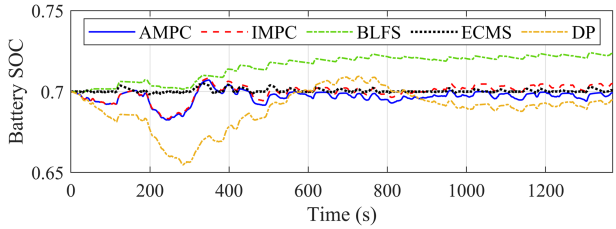

Fig. 13. Battery SOC curves using the five EMSs under the UDDS cycle.

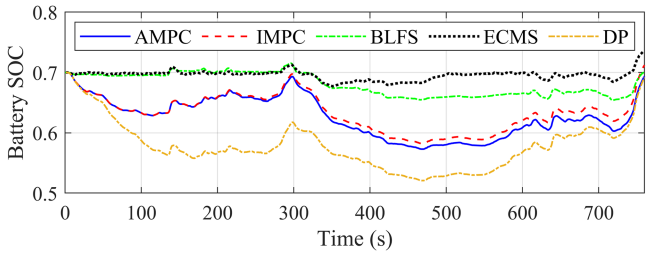

Fig. 14. Battery SOC curves using the five EMSs under the HWFET cycle.

ECMS is larger than that using the other three real-time EMSs. For the BLFS, the variation of the FC power is constrained by its boundary values, which are determined by the rule used in [40]. The offline DP-based EMS can optimize the objective function over the entire driving cycle and, thus, lead to smaller fluctuation of the FC output current than the other EMSs.

Figs. 13 and 14 compare the battery SOC curves using the five EMSs under the UDDS and HWFET cycle, respectively. All of the five EMSs can manage the hybrid FCS to sustain the charge of the battery and keep its SOC within the limits. The battery can store energy during the regenerative braking of the FCHEV.

Similar to [19] and [33], the five EMSs are further compared in terms of hydrogen energy consumption, FC current variation,

TABLE II
PERFORMANCE COMPARISON OF THE FOUR REAL-TIME EMSS

Cycle	Strategy	Hydrogen energy consumption [Wh]	FC current variation [A/s]	Final battery SOC [%]	Battery energy loss [Wh]	Battery energy consumption [Wh]	Total energy consumption [Wh]
UDDS	AMPC	23.06	0.0334	69.92	0.0156	0.0439	23.104
	IMPC	23.82	0.0355 (+6.29%)	70.49	0.0158	-0.287	23.533 (+1.86%)
	BLFS	26.52	0.765 (+2290.42%)	72.33	0.0203	-1.280	25.240 (+9.25%)
	ECMS	23.99	2.540 (+7604.79%)	70.05	0.0186	0.0006	23.991 (+3.84%)
HWFET	AMPC	167.67	0.131	69.49	0.205	0.331	168.031
	IMPC	171.62	0.145 (+10.69%)	71.38	0.217	-0.818	170.802 (+1.65%)
	BLFS	175.03	2.407 (+1837.40%)	70.06	0.241	0.220	175.250 (+4.30%)
	ECMS	183.49	9.357 (+7142.75%)	73.58	0.252	-1.898	181.592 (+8.07%)

battery energy loss, and battery SOC. The FC current variation σ is defined as follows:

$$\sigma = \sqrt{\frac{1}{N_s}\sum\nolimits_{k=1}^{N_s} \Delta I_{\mathrm{fc}}^2\left(k\right)} \tag{36}$$

where N_s is the total number of the sampling periods of a driving cycle. The hydrogen energy consumption E_{H2} in Wh can be calculated as follows [43]:

$$E_{\mathrm{H}_2} = \sum_{k=1}^{N_s} \dot{m}_{\mathrm{H}_2}\left(k\right) H_{\mathrm{LHV}} T \tag{37}$$

where H_{LHV} is the lower heating value of hydrogen in Wh/g. The battery energy consumption E_b is the sum of the battery output energy and battery energy loss over the cycle

$$E_b = \sum_{k=1}^{N_s} \left(V_b\left(k\right) I_b\left(k\right) + P_{b,\mathrm{Loss}}\left(k\right)\right) T/3600 \tag{38}$$

where V_b and I_b are measured by using sensors and $P_{b,\mathrm{Loss}}$ is calculated using (11). The total energy consumption E_t is then the sum of the hydrogen energy consumption and the battery energy consumption

$$E_t = E_{\mathrm{H}_2} + E_b. \tag{39}$$

Table II provides the performance comparison results of the four real-time EMSs. The AMPC-based EMS provides the best performance in reducing the total energy consumption and the FC current variation among the four real-time EMSs for the energy management of the FCHEV under both driving cycles. Compared with the IMPC, the AMPC achieved a 1.86%/1.65% reduction in the total energy consumption and a 6.29%/10.69% reduction in the FC current variation under the UDDS/HWFET driving cycle. The IMPC-based EMS uses a linear time-invariant model. As the operating condition of the FC hybrid system varies, the model-plant mismatch in the IMPC-based EMS leads to a degraded control performance. Since the control performance of MPC depends on the model quality, the proposed EMS achieved better performance than the IMPC-based EMS by updating the parameters of the prediction model in each sampling period based on the new state measurements and estimations.

Compared with the ECMS, the AMPC achieved a significant reduction of 7604.79%/7142.75% in the FC current variation under the UDDS/HWFET driving cycle. In addition, in contrast to the ECMS which only minimizes the instantaneous energy consumption at the current time step, the AMPC and IMPC minimize the total energy consumption over the entire prediction horizon. Thus, they offer better fuel economy than the ECMS, as shown in Table II.

TABLE III
PERFORMANCE COMPARISON OF THE REAL-TIME EMSS WITH THE OFFLINE DP-BASED OPTIMAL EMS

Cycle	Strategy	FC current variation	Total energy consumption
UDDS	AMPC	+0.22%	+3.53%
	IMPC	+0.26%	+5.45%
	BLFS	+14.85%	+13.10%
	ECMS	+50.35%	+7.50%
HWFET	AMPC	+0.94%	+1.50%
	IMPC	+1.22%	+3.17%
	BLFS	+46.46%	+5.86%
	ECMS	+185.46%	+9.69%

Compared with the BLFS, the AMPC achieved a 9.25%/4.30% reduction in the total energy consumption and a 2290.42%/1837.40% reduction in the FC current variation under the UDDS/HWFET driving cycle. Since the BLFS does not minimize the energy consumption, the total energy consumption performance achieved by the BLFS was the worst among the four real-time EMSs.

The LPV prediction model of the FC hybrid system allows the proposed EMS to consider the battery energy loss explicitly in the objective function. As shown in Table II, the proposed EMS achieved the least battery energy loss among the four real-time EMSs in both driving cycles.

Table III compares the performance deviations of the four real-time EMSs from the offline DP-based optimal EMS, where it was assumed that the exact information of the entire UDDS and HWFET driving cycles was known *a priori* when designing the DP-based EMS offline. The FC current variations are calculated as percentages with respect to the allowed limit of 5 A/s. The FC current variation and total consumption using the proposed AMPC-based EMS are only 0.22%/0.94% and 3.53%/1.50% larger than the optimal results obtained offline from the DP-based EMS under the UDDS/HWFET driving cycles, respectively. Compared to the three existing real-time EMSs, both the total energy consumption and FC current variation performance achieved by the proposed AMPC-based EMS in real time under both driving cycles are much closer to the

optimal results obtained offline by the DP-based EMS. The comparative study demonstrates the superiority of the proposed EMS over the other real-time EMSs for the real-time optimal energy management of the FCHEV.

VII. Conclusion

This article proposed a new real-time AMPC-based EMS for optimally splitting the load current of an FCHEV between the FC and the battery of the FC hybrid system to achieve a desired tradeoff among four performance metrics. The proposed EMS was based on an LPV prediction model of the FC hybrid system, which offered sufficient accuracy while ensuring real-time implementation of the AMPC. In each control cycle of the AMPC, the parameters of the LPV prediction model were updated online to adapt to the variations of the battery SOC, which reduced the model-plant mismatch for the FC hybrid system. Real-time simulation was employed to reveal the execution time of the proposed EMS under different prediction horizons. HIL tests were performed on a downscaled hybrid FCS with the AMPC-based EMS in comparison with three existing real-time EMSs, i.e., an IMPC-based EMS, a BLFS, and an ECMS, while using an offline DP-based optimal EMS as the benchmark. The HIL-testing-based comparative study results demonstrated that among the four real-time EMSs, the AMPC-based EMS achieved the best control performance in reducing total energy consumption and FC current variation and the smallest optimality gap with respect to the offline benchmark.

References

[1] S. N. Motapon, L.-A. Dessaint, and K. Al-Haddad, "A robust H_2-consumption-minimization-based energy management strategy for a fuel cell hybrid emergency power system of more electric aircraft," *IEEE Trans. Ind. Electron.*, vol. 61, no. 11, pp. 6148–6156, Nov. 2014.

[2] H. Chaoui, M. Kandidayeni, L. Boulon, S. Kelouwani, and H. Gualous, "Real-time parameter estimation of a fuel cell for remaining useful life assessment," *IEEE Trans. Power Electron.*, vol. 36, no. 7, pp. 7470–7479, Jul. 2021.

[3] H. N. Tran, T. Le, H. Jeong, S. Kim, and S. Choi, "A 300 kHz, 64 kW/L ZVT DC-DC converter for 800-V fuel cell electric vehicles," *IEEE Trans. Power Electron.*, vol. 37, no. 3, pp. 2993–3006, Mar. 2022.

[4] M. Kandidayeni, A. Macias, L. Boulon, and S. Kelouwani, "Efficiency upgrade of hybrid fuel cell vehicles' energy management strategies by online systemic management of fuel cell," *IEEE Trans. Ind. Electron.*, vol. 68, no. 6, pp. 4941–4953, Jun. 2021.

[5] S. Zhou, Z. Chen, D. Huang, and T. Lin, "Model prediction and rule based energy management strategy for a plug-in hybrid electric vehicle with hybrid energy storage system," *IEEE Trans. Power Electron*, vol. 36, no. 5, pp. 5926–5940, May 2021.

[6] Y. Han, Q. Li, T. Wang, W. Chen, and L. Ma, "Multisource coordination energy management strategy based on SOC consensus for a PEMFC-battery-supercapacitor hybrid tramway," *IEEE Trans. Veh. Technol.*, vol. 67, no. 1, pp. 296–305, Jan. 2018.

[7] C. Jia, W. Qiao, and L. Qu, "A cost-oriented control strategy for energy management of a dual-mode locomotive," in *Proc. IEEE Veh. Power Propulsion Conf.*, Dec. 2019, pp. 1–6.

[8] H. Hemi, J. Ghouili, and A. Cheriti, "A real time fuzzy logic power management strategy for a fuel cell vehicle," *Energy Convers. Manage.*, vol. 80, pp. 63–70, 2014.

[9] J. Chen, C. Xu, C. Wu, and W. Xu, "Adaptive fuzzy logic control of fuel-cell-battery hybrid systems for electric vehicles," *IEEE Trans. Ind. Inform.*, vol. 14, no. 1, pp. 292–300, Jan. 2018.

[10] Q. Li, W. Chen, Z. Liu, M. Li, and L. Ma, "Development of energy management system based on a power sharing strategy for a fuel cell-battery-supercapacitor hybrid tramway," *J. Power Sources*, vol. 279, pp. 267–280, Dec. 2015.

[11] J. Snoussi, S. Elghali, M. Benbouzid, and M. Mimouni, "Auto-adaptive filtering-based energy management strategy for fuel cell hybrid electric vehicles," *Energies*, vol. 11, Aug. 2018, Art. no. 2118.

[12] C. Zhao, H. Yin, and C. Ma, "Equivalent series resistance-based real-time control of battery-ultracapacitor hybrid energy storage systems," *IEEE Trans. Ind. Electron.*, vol. 67, no. 3, pp. 1999–2008, Mar. 2020.

[13] W. Zhou, L. Yang, Y. Cai, and T. Ying, "Dynamic programming for new energy vehicles based on their work modes Part II: Fuel cell electric vehicles," *J. Power Sources*, vol. 407, pp. 92–104, 2018.

[14] A. Biswas and A. Emadi, "Energy management systems for electrified power trains: State-of-the-art review and future trends," *IEEE Trans. Veh. Technol.*, vol. 68, no. 7, pp. 6453–6467, Jul. 2019.

[15] X. Hu, N. Murgovski, L. M. Johannesson, and B. Egardt, "Optimal dimensioning and power management of a fuel cell/battery hybrid bus via convex programming," *IEEE/ASME Trans. Mechatron.*, vol. 20, no. 1, pp. 457–468, Feb. 2015.

[16] X. Hu, C. Zou, X. Tang, T. Liu, and L. Hu, "Cost-optimal energy management of hybrid electric vehicles using fuel cell/battery health-aware predictive control," *IEEE Trans. Power Electron.*, vol. 35, no. 1, pp. 382–392, Jan. 2020.

[17] W. Greenwell and A. Vahidi, "Predictive control of voltage and current in a fuel cell-ultracapacitor hybrid," *IEEE Trans. Ind. Electron.*, vol. 57, no. 6, pp. 1954–1964, Jun. 2010.

[18] D. F. Pereira, F. C. Lopes, and E. H. Watanabe, "Nonlinear model predictive control for the energy management of fuel cell hybrid electric vehicles in real time," *IEEE Trans. Ind. Electron.*, vol. 68, no. 4, pp. 3213–3223, Apr. 2021.

[19] H. Chen, J. Chen, H. Lu, C. Yan, and Z. Liu, "A modified MPC-based optimal strategy of power management for fuel cell hybrid vehicles," *IEEE/ASME Trans. Mechatron.*, vol. 25, no. 4, pp. 2009–2018, Aug. 2020.

[20] H. He, S. Quan, F. Sun, and Y. Wang, "Model predictive control with lifetime constraints based energy management strategy for proton exchange membrane fuel cell hybrid power systems," *IEEE Trans. Ind. Electron.*, vol. 67, no. 10, pp. 9012–9023, Oct. 2020.

[21] Y. Zhou, A. Ravey, and M. Pera, "Multi-mode predictive energy management for fuel cell hybrid electric vehicles using Markov driving pattern recognizer," *Appl. Energy*, vol. 258, 2020, Art. no. 114057.

[22] D. Shen, C. Lim, and P. Shi, "Robust fuzzy model predictive control for energy management systems in fuel cell vehicles," *Control Eng. Pract.*, vol. 98, 2020, Art. no. 104364.

[23] D. Q. Mayne, J. B. Rawlings, C. V. Rao, and P. M. Scokaert, "Constrained model predictive control: Stability and optimality," *Automatica*, vol. 36, pp. 789–814, 2000.

[24] M. Morato, J. Normey-Rico, and O. Sename, "Model predictive control design for linear parameter varying systems: A survey," *Annu. Rev. Control*, vol. 49, pp. 64–80, 2020.

[25] L. Zhang and N. Wang, "An adaptive RNA genetic algorithm for modeling of proton exchange membrane fuel cells," *Int. J. Hydrogen Energy*, vol. 38, pp. 219–228, 2013.

[26] M. Kandidayeni, A. M. Fernandez, A. Khalatbarisoltani, L. Boulon, S. Kelouwani, and H. Chaoui, "An online energy management strategy for a fuel cell/battery vehicle considering the driving pattern and performance drift impacts," *IEEE Trans. Veh. Technol.*, vol. 68, no. 12, pp. 11427–11438, Dec. 2019.

[27] W. Lhomme et al., "IEEE VTS motor vehicle challenge 2019—Energy management of a dual-mode locomotive," in *Proc. IEEE Veh. Power Propulsion Conf.*, Aug. 2018, pp. 1–6.

[28] C. Lin, H. Mu, R. Xiong, and W. Shen, "A novel multi-model probability battery state of charge estimation approach for electric vehicles using H-infinity algorithm," *Appl. Energy*, vol. 166, pp. 76–83, 2016.

[29] H. He, R. Xiong, X. Zhang, F. Sun, and J. Fan, "State-of-charge estimation of the Lithium-ion battery using an adaptive extended Kalman filter based on an improved Thevenin model," *IEEE Trans. Veh. Technol.*, vol. 60, no. 4, pp. 1461–1469, May 2011.

[30] G. L. Plett, "Extended Kalman filter for battery management systems of LiPB-based HEV battery packs Part 3. State and parameter estimation," *J. Power Source*, vol. 134, pp. 277–292, 2004.

[31] B. Geng, J. K. Mills, and D. Sun, "Two-stage energy management control of fuel cell plug-in hybrid electric vehicles considering fuel cell longevity," *IEEE Trans. Veh. Technol.*, vol. 61, no. 2, pp. 498–508, Feb. 2012.

[32] L. Wang, Y. Wang, C. Liu, D. Yang, and Z. Chen, "A power distribution strategy for hybrid energy storage system using adaptive model predictive control," *IEEE Trans. Power Electron.*, vol. 35, no. 5, pp. 5897–5906, Jun. 2020.
[33] C. Wu, J. Chen, C. Xu, and Z. Liu, "Real-time adaptive control of a fuel cell/battery hybrid power system with guaranteed stability," *IEEE Trans. Control Syst. Technol.*, vol. 25, no. 4, pp. 1394–1405, Jul. 2017.
[34] L. Cavanini, G. Ippoliti, and E. F. Camacho, "Model predictive control for a linear parameter varying model of an UAV," *J. Intell. Robot. Syst.*, vol. 101, no. 57, pp. 1–18, 2021.
[35] A. Khalatbarisoltani, M. Kandidayeni, L. Boulon, and X. Hu, "Power allocation strategy based on decentralized convex optimization in modular fuel cell systems for vehicular applications," *IEEE Trans. Veh. Technol.*, vol. 69, no. 12, pp. 14563–14574, Dec. 2020.
[36] P. Cortes et al., "Guidelines for weighting factors design in model predictive control of power converters and drives," in *Proc. IEEE Int. Conf. Ind. Technol.*, Feb. 2009, pp. 1–7.
[37] C. Jia, J. Cui, W. Qiao, and L. Qu, "A reduced-scale power hardware-in-the-loop platform for fuel cell electric vehicles," in *Proc. IEEE Transp. Electrific. Conf. Expo.*, Jun. 2021, pp. 1–6.
[38] C. Jia, W. Qiao, and L. Qu, "Numerical methods for optimal control of hybrid electric agricultural tractors," in *Proc. IEEE Transp. Electrific. Conf. Expo*, Jun. 2019, pp. 1–6.
[39] P. Elbert, S. Ebbesen, and L. Guzzella, "Implementation of dynamic programming for n-dimensional optimal problem with final state constraints," *IEEE Trans. Control Syst. Technol.*, vol. 21, no. 3, pp. 924–931, May 2013.
[40] M. Carignano, V. Roda, R. Costa-Castelló, L. Valiño, A. Lozano, and F. Barreras, "Assessment of energy management in a fuel cell/battery hybrid vehicle," *IEEE Access*, vol. 7, pp. 16110–16122, 2019.
[41] R. Kumar et al., "Revealing the benefits of entropy weights method for multi-objective optimization in machining operations: A critical review," *J. Mater. Res. Technol.*, vol. 10, pp. 1471–1492, 2021.
[42] M. Li, L. Wang, Y. Wang, and Z. Chen, "Sizing optimization and energy management strategy for hybrid energy storage system using multiobjective optimization and random forests," *IEEE Trans. Power Electron.*, vol. 36, no. 10, pp. 11421–11430, Oct. 2021.
[43] Y. Zhang et al., "Improved short-term speed prediction using spatiotemporal-vision-based deep neural network for intelligent fuel cell vehicles," *IEEE Trans. Ind. Inform.*, vol. 17, no. 9, pp. 6004–6013, Sep. 2021.

Chao Jia (Member, IEEE) received the B.Eng. degree in mechanical engineering and the M.Eng. degree in electrical engineering from Beijing Institute of Technology, Beijing, China, in 2012 and 2016, respectively, and the Ph.D. degree in electrical engineering from the University of Nebraska–Lincoln, Lincoln, NE, USA, in 2022.

He is currently a Postdoctoral Associate with the Department of Electrical and Computer Engineering, University of Nebraska–Lincoln. His research interests include energy management of hybrid electric vehicles and energy storage systems.

Dr. Jia was the second-place winner of the IEEE VTS Motor Vehicle Challenge 2019.

Wei Qiao (Fellow, IEEE) received the B.Eng. and M.Eng. degrees in electrical engineering from Zhejiang University, Hangzhou, China, in 1997 and 2002, respectively, the M.S. degree in high-performance computation for engineered systems from Singapore-MIT Alliance, Singapore, in 2003, and the Ph.D. degree in electrical engineering from the Georgia Institute of Technology, Atlanta, GA, USA, in 2008.

Since August 2008, he has been with the University of Nebraska–Lincoln, Lincoln, NE, USA, where he is currently the Clyde Hyde Professor of Electrical and Computer Engineering. He has authored or coauthored more than 270 papers in refereed journals and conference proceedings and holds 11 U.S. patents issued. His research interests include modeling, control, condition monitoring, and optimization of renewable energy systems, power electronic systems, electric motor drives, energy storage systems, electric vehicles, and electric power grids; decision making and risk management in the electricity markets with high penetrations of renewable energy; and electrical energy conversion devices.

Prof. Qiao was a recipient of the 2010 U.S. National Science Foundation CAREER Award, and the recipient of the 2021 IEEE Power Electronics Society Sustainable Energy Systems Technical Achievement Award and the 2010 IEEE Industry Applications Society Andrew W. Smith Outstanding Young Member Award.

Junwei Cui (Member, IEEE) received the B.Eng. degree from North University of China, Shanxi, China, in 2003, the M.Eng. degree from Shanghai Jiaotong University, Shanghai, China, in 2007, and the Ph.D. degree from the University of Nebraska–Lincoln, Lincoln, NE, USA, in 2022, all in electrical engineering.

From 2007 to 2016, he was an Electrical Engineer in GE Renewable, responsible for power transformer and switchgear with the GE China Technology Center, Shanghai, China. He is currently a Senior Power Electronics Electrical Engineer with the BorgWarner Inc, Auburn Hills, MI, USA. His research interests include magnetic devices, power electronics, and electric power conversion.

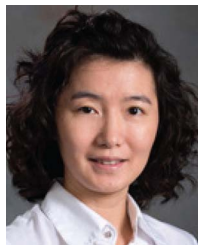

Liyan Qu (Senior Member, IEEE) received the B.Eng. (with the highest distinction) and M.Eng. degrees in electrical engineering from Zhejiang University, Hangzhou, China, in 1999 and 2002, respectively, and the Ph.D. degree in electrical engineering from the University of Illinois at Urbana–Champaign, Champaign, IL, USA, in 2007.

From 2007 to 2009, she was an Application Engineer with Ansoft Corporation, Irvine, CA, USA. Since January 2010, she has been with the University of Nebraska−Lincoln, Lincoln, NE, USA, where she is currently an Associate Professor with the Department of Electrical and Computer Engineering. Her research interests include energy efficiency, renewable energy, numerical analysis and computer-aided design of electric machinery and power electronic devices, dynamics and control of electric machinery, and magnetic devices.

Dr. Qu was a recipient of the 2016 U.S. National Science Foundation CAREER Award.